PREDICTION OF MECHANICAL PROPERTIES OF QUENCH HARDENING STEEL*

R. Chotěborský, M. Linda

Czech University of Life Sciences Prague, Faculty of Engineering, Prague, Czech Republic

The present study investigated the application of finite element method for prediction of mechanical properties of quench hardening steel. Based on the experimental results obtained, a numerical model for simulation of continuous cooling of quench hardening steel was developed. For the simulation of the kinetics of diffusion phase transformations, the Avrami equation and additive rule were applied. A new model was also developed for martensitic transformation which was validated using metallographic analysis and hardness tests. Experimental and simulation results indicated a good agreement. The developed model information provided here could be used for simulation of continuous cooling and kinetics phase transformation as well as for prediction of final distribution of microstructures and hardness of alloy steels.

finite element model; heat flux; microstructure; hardness; continuous cooling

DE GRUYTER OPEN

doi: 10.1515/sab-2015-0013
Received for publication on March 24, 2014
Accepted for publication on January 14, 2015

INTRODUCTION

Quenching is a thermal process frequently used to obtain good mechanical properties of steel and other metal alloy materials. The quenching application of the material is subjected to heat treatment above the austenitization temperature (approximately 900°C) involving continuous and rapid cooling in a quenching media including water, air, and oil (Chotěborský, 2013). Based on the heat treatment of the material, Sugianto et al. (2009) compared two different techniques of heat transfer capacity (HTC) determination. These include the lumped heat capacity method and the inverse heat transfer method. Buczek, Telejko (2004) performed experiments under various cooling conditions through position of the active surface of the sample, its initial temperature and water temperature. Heat transfer of the sample–quenchant interface in other media than water was investigated using brine, water, mineral, and palm oils and other vegetable oils (Fernandes, Prabhu, 2007, 2008). Quenching fluids such as polymer–water solutions and nanofluids have also been used by some authors (Coursey et al., 2008; Babu, Prasanna Kumar, 2011; Eshraghi-Kakhki et al., 2011). However, the quenching fluids that have been used were defined by the quenchant temperature and the heat transfer coefficient at the cooling surface. During quench hardening, heat flux transfers rapidly to the coolant which varies in time, hence the HTC cannot be calculated or measured by standard techniques. In such cases, the most suitable procedure is the formulation of the boundary inverse heat conduction (Buczek, Telejko, 2013). This method consists of numerical selection of boundary conditions to provide temperature distribution in the material within limits of accuracy based on known data. The temperature profile is measured by sensors placed at selected internal points of the material during cooling. To determine the heat transfer coefficients of the material at the cooling surface, lumped heat capacity approximate technique has been applied at constant work piece temperature. Kobasko et al. (2004) experimentally determined the first and second critical heat flux densities to characterize the quenching process. Most useful method for obtaining the realistic metal/quenchant interfacial heat transfer properties is the inverse modelling which allows the determination of boundary conditions by the coupling of numerical methods with simple temperature measurements inside the quench probe. The objective of

* Supported by the Internal Grant Agency of the Faculty of Engineering, Czech University of Life Sciences Prague (IGA), Project No. 2014: 31200/1312/3130.

this study was to investigate the possibility of using finite element method for prediction of mechanical properties of quench hardening steel.

MATERIAL AND METHODS

The experiment was carried out using the vertical furnace for the samples heating, quenching media (water, oil, and salt bath) for cooling the samples, thermocouple K-type for temperature measurement, and Scilab software (Version 5.4.1, 2012) for data processing. Samples were heated in an electrical furnace LMV2/10 (LAC, s.r.o., Rajhrad, Czech Republic) for 1 h and cooled in a quenching media including water, oil, and salt bath ($NaNO_3 + NaNO_2$). Quenched samples were cut into cross sections for hardness measurement using Vickers tester of 30 kg load. The cut samples were placed in core diameters 3, 7, and 11 mm respectively under the surface of the cylinder. For the temperature measurement, the thermocouple was cast into two parts 1 and 2 (CSN 41 4260 (414260) Steel 14 260 Si-Cr: 03/1988) (Fig. 1). Thermocouple 1 was placed 2 mm below the surface of the cylinder while thermocouple 2 was placed on the axis of the cylinder. Temperature measurement by thermocouple 2 was used to evaluate the results obtained. Thermocouple 1 temperature measurement was used for resolving the inverse problem of nonlinear heat conduction equation. The measured data was analyzed using the computer program Scilab (Version 5.4.1., 2012).

Mathematical models

The equations described below were used for the experimental data evaluation. Eq.1 is a one-dimensional transient heat conduction equation based on cylindrical coordinates.

$$\rho \times C_p \times \frac{\partial T}{\partial t} = \frac{k}{r} \times \frac{\partial}{\partial r}\left(r \times \frac{\partial T}{\partial r}\right) \quad (1)$$

where:

k = thermal conductivity ($W.m^{-1}.K^{-1}$)

r = density ($kg.m^{-3}$)

C_p = specific heat capacity ($J.kg^{-1}.K^{-1}$) of the quenched sample

Eq.1 was solved inversely but the details of the inverse analysis were described by Prabhu et al. (2003), Fernandes et al. (2007), and Cao et al. (2012). The experimental heat flow was also determined by Eq. 2.

$$\Phi_q = \frac{\Delta T}{\Delta t} \times C_p(T) \quad (2)$$

The boundary conditions of the model were determined with respect to the outward normal vector n:

$$\frac{\partial T}{\partial n}(x,t) = -\frac{\Phi_q(x,t)}{\lambda} \quad (3)$$

The Elmer FEM solver software (Version 7.0, 2008) was used for the thermal field determination of samples. The simulation results were obtained as a matrix of nodes and temperature. In the literature (Smoljan, 2006; Malinowski et al., 2012), two kinds of mathematical models have been established for evaluation of microstructure field from temperature field based on TTT (Time, Temperature, Transformation) curve which is used for kinetic transformation of austenite at constant temperature and CCT (Continuous Cooling Transformation) curve which is also used for kinetic transformation of austenite in a water and oil quenching media. The transformations towards pearlite and bainite are both diffusive phase transformations. The Avrami formula which describes the transformation volume is:

$$V_{P,B} = 1 - e^{-k \times t^n} \quad (4)$$

where:

k = overall rate constant dependent on temperature

n = Avrami exponent

The transformation towards martensite is a non-diffusive transformation adopted by the model of Koistinen, Marburger (1959) which describes the transformation volume as:

$$V_M = 1 - e^{-\alpha \times (M_s - T)} \quad (5)$$

where α and M_s are both constants based on material type. The actual temperature variation is a continuous cooling rather than isothermal variation. But austenite phase under M_s temperature can be partially transformed to bainite. By applying the Scheil superposition principle, actual continuous cooling transformation can be

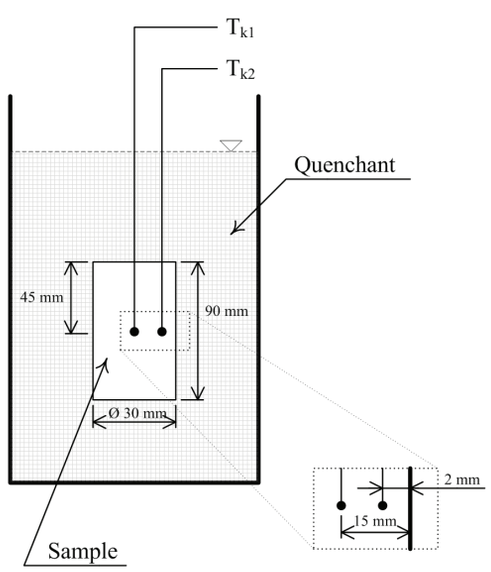

Fig. 1. Scheme of the experiment procedure, sample and thermocouples

determined by the isothermal transformation model. Here the time period was discretized based on the assumption that within each time step is Δt at constant temperature involving the isothermal transformation.

Dividing the time step Δt by incubation period τ_i produced the increment of inoculation rate ΔE_i which was the volume transformation during the former time step V_i. Substituting this into Eq. 6, then the time period can be obtained from the volume transformation V_i under T_{i+1} isothermal transformation condition that is the virtual time t_{i+1} as described below.

$$t_{i+1} = \left[\frac{-\ln(1-V_i)}{k_{i+1}}\right]^{\frac{1}{n_{i+1}}} \tag{6}$$

Coefficients k and n in Eq. 4 as well as α and M_s in Eq. 5 were determined experimentally based on the method described by Cao et al. (2012). Microstructures were calculated from arrays {T (t)} and {V (t)} during the simulation period. Mechanical properties of quenched steel or quenched and tempered steel directly depended on the degree of quenched steel hardening. Relationship between hardness (HV) and ultimate tensile stress (R_m) can be described as:

$$R_m = 3.3 \times HV \tag{7}$$

Yield strength can be estimated based on the ultimate stress or hardness equation as described below:

$$R_e = R_{p0.2} = 0.8 \times R_m + 170 \times C - 200 \tag{8}$$

where C is the ratio between the actual hardness and martensite hardness. Structural composition of steel influences actual steel hardness which is generally described by the equation:

$$HV = V_p \times HV_p + V_B \times HV_B + V_M \times HV_M \tag{9}$$

According to Maynier's study (Maynier et al., 1977), based on Eq. 9 can be fitted total hardness value, where the Eqs 10-12 can describe hardness of each phase which were set through series of experiments involving different kinds of alloy steel:

$$HV_M = 127 + 949 \times C + 27 \times Si + 8 \times Ni + 16 \times Cr + \\ + 21 \times \ln V_r \tag{10}$$

$$HV_B = -323 + 185 \times C + 330 \times Si + 153 \times Mn + \\ + 65 \times Ni + 144 \times Cr + 191 \times Mo + (89 + 53 \times C - \\ - 55 \times Si - 22 \times Mn - 10 \times Ni - 20 \times Cr - 33 \times Mo) \times \\ \times \ln V_r \tag{11}$$

$$HV_{F,B} = 42 + 233 \times C + 53 \times Si + 30 \times Mn + \\ + 12.6 \times Ni + 7 \times Cr + 19 \times Mo + (10 - 19 \times Si + \\ + 4 \times Ni + 8 \times Cr + 130 \times V) \times \ln V_r \tag{12}$$

where C, Si, Mn and others represent different kinds of chemical elements (wt. %), V_r represents cooling speed at 700°C (°C.h^{-1}).

Eqs. 13–15 were used in the finite element method model to fit the experimental data:

$$\Phi_q(T)_{water} = -0.0026 \times T^3 - 0.8202 \times T^2 + \\ + 2937 \times T + 2 \times 10^6 \tag{13}$$

$$\Phi_q(T)_{oil} = -0.0248 \times T^3 + 25.4 \times T^2 - 3739 \times T + \\ + 2.5 \times 10^5 \tag{14}$$

$$\Phi_q(T)_{salt} = -0.00003 \times T^4 + 0.0548 \times T^3 - 33.9 \times T^2 - \\ - 9858 \times T + 34066 \tag{15}$$

where T is the surface temperature (°C) which was obtained for each quenchant. The fitted curve was based on the heat flux boundary conditions.

RESULTS

Fig. 2 shows the thermal properties and cooling rates of CSN 41 4260: 1988 steel measured at the core of samples diameter 2 mm from the interface which was subjected to quenching in water with agitation within a time span of 21 s. The temperature measurement was previously used as input for the inverse heat conduction model which was used to estimate the heat flux transients at the metal/quenchant interface. The inverse analysis yielded the surface temperature of the samples in contact with the quenching media. Fig. 3 shows the relationship between the estimated heat flux and the surface temperature of steel. The heat flux value was lower in the initial period of quenching

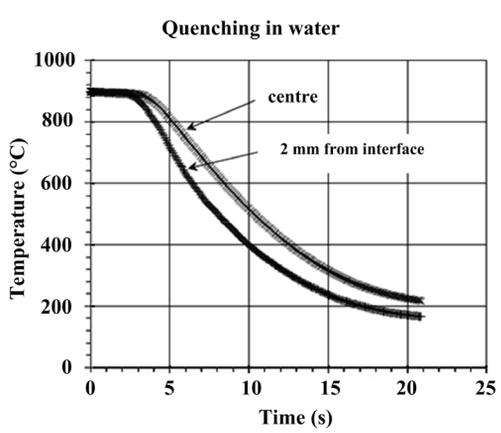

Fig. 2. Relationship between temperature and time of steel quenched in water

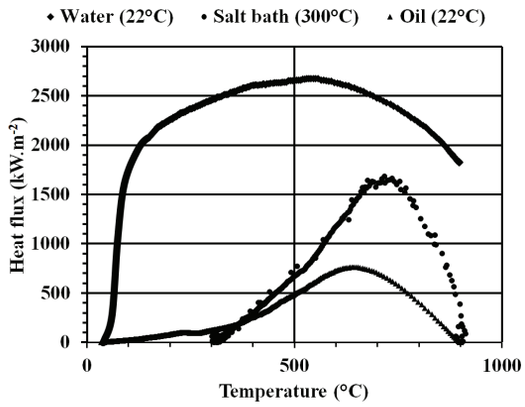

Fig. 3. Relationship between heat flux and surface temperature of various quenching media

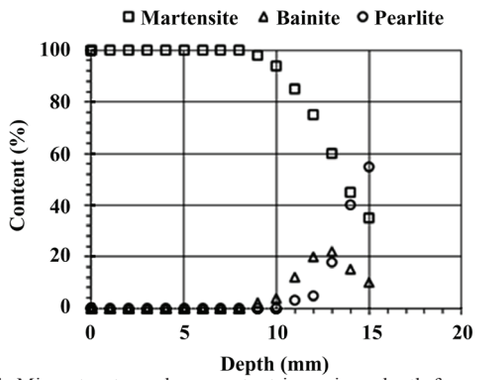

Fig. 4. Microstructure phase content in various depth from surface, quenchant-water

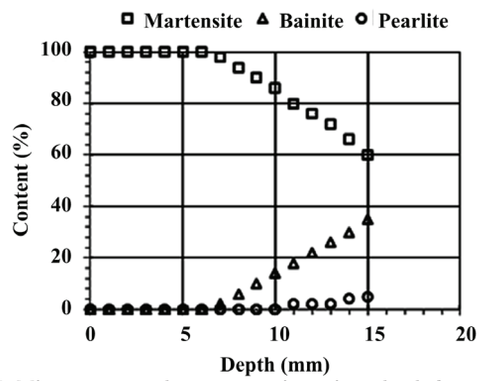

Fig. 5. Microstructure phase content in various depth from surface, quenchant-oil

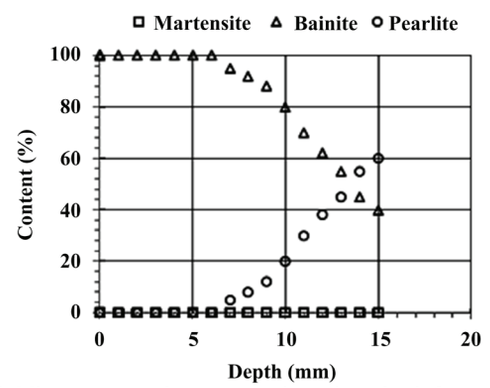

Fig. 6. Microstructure phase content in various depth from surface, quenchant-salt bath

due to the vapour film formed at the surface of the steel samples. The vapour film actually offers some resistance to heat transfer as a result of insulation effect and low thermal conductivity. As the quenching process progressed, the vapour film disrupted allowing the rate of heat transfer to increase intensively (H e m i n g et al., 2003). The duration of vapour blanket stage was decreased during the agitation of quenching media (K i m , O h , 2001). The heat flux transients increased rapidly due to enhanced convective heat transfer between the samples and quenching media. The heat flux transients showed a peak during nucleate boiling stage in quenching media and the occurrence of peak in the heat flux associated with the peak thermal gradient existing inside the quenched samples with complete cessation of the vapour film. Peak heat flux value (Fig. 3) was obtained for water media with 30 mm diameter at 550°C and 650°C for oil, and 720°C for salt bath. Eqs. 4–6 were used for the various microstructure predictions dependent on depth of quenchant as presented in Figs. 4–6. Fig. 7 represents the relationship of hardness and depth of various quenchants according to Eq. 9. Fig. 8 shows values of the strength of steel in water quenching medium using Eqs. 7 and 8. Fig. 9 represents the relationship between hardness measured and hardness model of steel for quenching media of water, oil, and salt. It was observed that modelled data attained higher values than the measured ones (Fig. 9).

DISCUSSION

For the various quenching media (water, oil, and salt) used in the study, the maximum heat flux value obtained was lower compared to previously published results (P r a b h u , P r a s a d , 2003; F e r n a n d e z , P r a b h u , 2007; B a b u , P r a s a n n a K u m a r , 2011, a.o.). Briefly, F e r n a n d e z , P r a b h u (2007) found maximum heat flux value of 2500 kW.m^{-2} for water at 450°C surface temperature which was contrary to the present study results recorded as 2700 kW.m^{-2} at 550°C. The difference of 100°C could be attributed to the diameter of the sample used. These authors also indicated maximum heat flux of 1000 kW.m^{-2} at 550°C which was different from the present study result. In this study the authors used carbon steel and stainless steel due to their high amount of chromium composition. However, chemical composition of steel can lead to different heat flux and surface temperature values. In the case of oil quenching media, according to F e r n a n d e z , P r a b h u (2007) and B a b u ,

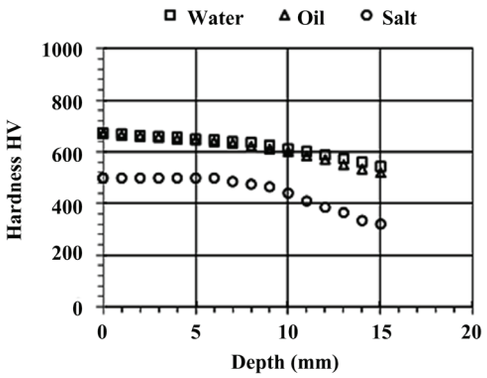

Fig. 7. Relationship between hardness and depth for various quenchant

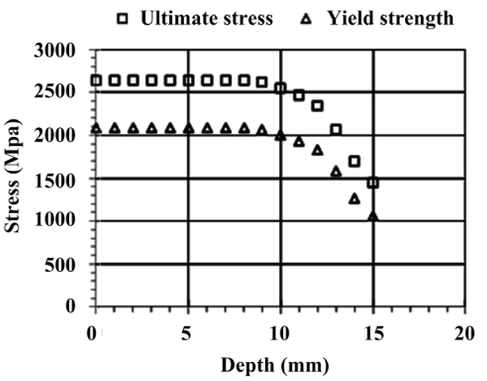

Fig. 8. Relationship between Ultimate stress and Yield strength in various depth for water quenching media

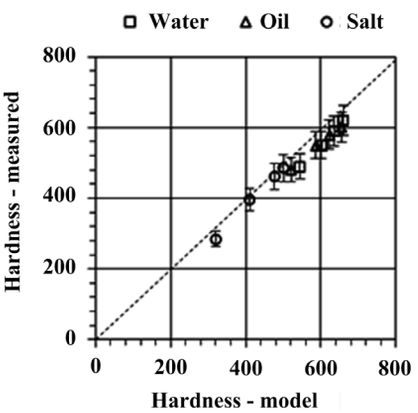

Prasanna Kumar (2011) the maximum heat flux was 1750 kW.m^{-2} at 520°C being higher than the present result which was found to be 750 kW.m^{-2} at 650°C. Buczek, Telejko (2013) found slightly similar result between 2000 and 3000 kW.m^{-2} at 530°C. By comparison, the heat flux in the oil depended on chemical composition of oil and temperature. For salt in the liquid state at 300°C, the maximal heat flux was 1750 kW.m^{-2} at 720°C. Generally, in the literature, the heat flux value is maximal both in water and oil quenching media than in salt. The relationship between heat flux and surface temperature produced error in modelling computation. The Avrami equation for kinetic transformation of austenite has been used by some authors (Maynier et al., 1977; Smoljan, 2006). Nucleation and saturation of transformed phase are described in the Avrami equation by coefficient *n* in the range of 0–5. If *n* is smaller, the nucleation rate is faster and saturation time is longer. Contrarily, if *n* is higher, the nucleation rate is slower and saturation time is shorter. This is because the nucleation and saturation transformation phases are dependent on chemical composition and austenite grain size. Therefore, it is necessary to consider suitable conditions for phase transformation. In the literature, some authors have reported the use of experimental dilatometer procedure (Jung et al., 2012) or FEM modelling of phase kinetics (Pernach, Pietrzyk, 2008; Yeddu et al., 2012). Implementation of the FEM model is not possible in this case because computation procedure requires a computer cluster with a very high computation power. For the experimental procedure, an electromagnetic principle was used where inductance of the measured object was dependent on the volume of magnetic phase (Liu et al., 2012; Chotěborský et al., 2014). The results show that the transformation of phase kinetics can be described by an electromagnetic method and this method is applicable by finding the value of coefficient *n* in the Avrami equation. The final model for prediction of microstructure and mechanical properties has been used by Liu et al. (2003), Simsir, Gür (2008), and Lee et al. (2010, 2013). The same decomposition system was successfully used in the present study. There were some slight differences between the modelled and the measured values of mechanical properties of quench hardening steel which are acceptable in the literature. However, relative value differences are similar to the results published by Huiping et al. (2007), Cao et al. (2012), Jung et al. (2012). The application of one dimensional equation instead of a generalized equation (2D or 3D) is due to the cylindrical shape of the sample. The one dimensional equation is useful for experimental and model evaluation.

CONCLUSION

Quenching the samples in water produced 100% martensite at the surface of the steel samples where the thickness of the hardening layer was found to be 8 mm. Lower hardenability was observed in oil quenching with a 6 mm thickness of the hardening layer. Quenching the steel samples in salt bath showed non-martensite transformation but produced a bainitic structure. Bainite was produced at the surface of the steel sample where the observed thickness of the bainite layer was 6 mm. Tempering of the steel samples decreased hardness while toughness increased. Martensite microstructure was produced from the steel tempering process. The light microscopic observation of the steel samples showed similar phase ratio to

that of the model predicted values. But determination of phase ratio for bainitic and martensitic structures was difficult due to similar morphology of the light microscopy. Measured hardness values were close to the modelled hardness which indicates the reliability of the model for prediction of mechanical properties of quenched hardening steels.

REFERENCES

Babu K, Prasanna Kumar TS (2011): Effect of CNT concentration and agitation on surface heat flux during quenching in CNT nanofluids. International Journal of Heat Mass Transfer, 54, 106–117. doi: 10.1016/j.ijheatmasstransfer.2010.10.003.

Buczek A, Telejko T (2004): Inverse determination of boundary conditions during boiling water heat transfer in quenching operation. Journal of Materials Processing Technology, 155–165, 1324–1329. doi: 10.1016/j.jmatprotec.2004.04.192.

Buczek A, Telejko T (2013): Investigation of heat transfer coefficient during quenching in various cooling agents. International Journal of Heat and Fluid Flow, 44, 258–264. doi: 10.1016/j.ijheatfluidflow.2013.07.004.

Cao P, Liu G, Wu K (2012): Numerical simulation and analysis of heat treatment of large-scale hydraulic steel gate track. International Journal of Material and Mechanical Engineering, 1, 16–20. doi: 10.3882/j.issn.1674-2370.2013.04.006.

Chotěborský R (2013): Effect of heat treatment on the microstructure, hardness and abrasive wear resistance of high chromium hardfacing. Research in Agricultural Engineering, 59, 23–28.

Chotěborský R, Linda M, Ružbarský J, Müller M (2014): Modelling of the anisothermal phase transformation of austenite by electromagnetic sensor. Applied Mechanics and Materials, 616, 44–51.

Coursey JS, Weng CI, Lin J (2008): Nanofluid boiling: the effect of surface wettability. International Journal of Heat and Fluid Flow, 29, 1577–1585.

Eshraghi-Kakhki M, Golozar MA, Kermanpur A (2011): Application of polymeric quenchant in heat treatment of crack-sensitive steel mechanical parts: modeling and experiments. Materials and Design, 32, 2870–2877. doi: 10.1016/j.matdes.2010.12.023.

Fernandes P, Prabhu KN (2007): Effect of section size and agitation on heat transfer during quenching of AISI 1040 steel. Journal of Materials Processing Technology, 183, 1–5. doi: 10.1016/j.jmatprotec.2006.08.028.

Fernandes P, Prabhu KN (2008): Comparative study of heat transfer and wetting behaviour of conventional and bioquenchants for industrial heat treatment. International Journal of Heat Mass Transfer, 51, 526–538. doi: 10.1016/j.ijheatmasstransfer.2007.05.018.

Heming C, Xieqing H, Jianbin X (2003): Comparison of surface heat transfer coefficient between various diameter cylinders using rapid cooling. Journal of Materials Processing Technology, 138, 399–402. doi: 10.1016/S0924-0136(03)00106-7.

Huiping L, Guoqun Z, Shanting H, Chuanzhen H (2007): FEM simulation of quenching process and experimental verification of simulation results. Materials Science and Engineering: A, 452–453, 705–714. doi:10.1016/j.msea.2006.11.023.

Jung M, Kang M, Kook-Lee Y (2012): Finite-element simulation of quenching incorporating improved transformation kinetics in a plain medium-carbon steel. Acta Materialia, 60, 525–536. doi: 10.1016/j.actamat.2011.10.007.

Kim HK, Oh SI (2001): Evaluation of heat transfer coefficient during heat treatment by inverse analysis. Journal of Materials Processing Technology, 112, 157–165. doi: 10.1016/S0924-0136(00)00877-3.

Kobasko NI, Aronov MA, Powel JA, Canale LCF, Totten GE (2004): Intensive quenching process classification and application. Heat Treatment of Metals, 31, 51–58.

Koistinen DP, Marburger RE (1959): A general equation prescribing the extent of the austenite-martensite transformation in pure iron-carbon alloys and plain carbon steels. Acta Metallurgica, 7, 59–60.

Lee S-J, Pavlina EJ, Van Tyne CJ (2010): Kinetics modeling of austenite decomposition for an end-quenched 1045 steel. Materials Science and Engineering: A, 527, 3186–3194. doi:10.1016/j.msea.2010.01.081.

Lee S-J, Matlock DK, Van Tyne CJ (2013): Comparison of two finite element simulation codes used to model the carburizing of steel. Computational Materials Science, 68, 47–54. doi:10.1016/j.commatsci.2012.10.007.

Liu CC, Xu XJ, Liu Z (2003): A FEM modeling of quenching and tempering and its application in industrial engineering. Finite Elements in Analysis and Design, 39, 1053–1070. doi: 10.1016/S0168-874X(02)00156-7.

Liu J, Hao XJ, Zhou L, Strangwood M, Davis CL, Peyton AJ (2012): Measurement of microstructure changes in 9Cr-1Mo and 2.25Cr-1Mo steels using an electromagnetic sensor. Scripta Materialia, 66, 367–370. doi:10.1016/j.scriptamat.2011.11.032.

Malinowski Y, Telejko T, Hadala B (2012): Influence of heat transfer boundary conditions on the temperature field of the continuous cast ingot. Archives of Metallurgy and Materials, 57, 325–331.

Maynier P, Dollet J, Bastien P (1977): Prediction of microstructure via empirical formulae based on CCT diagrams. Hardenability concepts with applications to steel, 163-178.

Pernach M, Pietrzyk M (2008): Numerical solution of the diffusion equation with moving boundary applied to modelling of the austenite-ferite phase transformation. Computation Materials Science, 44, 783–791.

Prabhu KN, Prasad A (2003): Metal/quenchant interfacial heat flux transients during quenching in conventional quench media and vegetable oils. Journal of Materials Engineering and Performance, 12, 48–55.

Simsir C, Gür C (2008): A FEM model based framework for simulation of thermal treatments: application to steel quenching. Computational Materials Science, 44, 588–600. doi: 10.1016/j.commatsci.2008.04.021.

Smoljan B (2006): Prediction of mechanical properties and microstructure distribution of quenched and tempered steel shaft. Journal of Materials Processing Technology, 175, 393–379. doi: 10.1016/j.jmatprotec.2005.04.068.

Sugianto A, Narazaki M, Kogawara M, Shirayori A (2009): A comparative study on determination method of heat transfer coefficient using inverse heat transfer and iterative modification. Journal of Materials Processing Technology, 209, 4627–4632. doi: 10.1016/j.jmatprotec.2008.10.016.

Yeddu HK, Malik A, Agren J, Amberg G, Borgenstam A (2012): Three-dimensional phase-field modeling of martensitic microstructure evolution in steels. Acta Materialia, 60, 1538–1547.

Corresponding Author:

Doc. Ing. Rostislav C h o t ě b o r s k ý , Ph.D., Czech University of Life Sciences Prague, Faculty of Engineering, Kamýcká 129, 165 21 Prague 6-Suchdol, Czech Republic, phone: +420 224 383 274, e-mail: choteborsky@tf.czu.cz